Food Hydrocolloids 134 (2023) 107975

Contents lists available at ScienceDirect

Food Hydrocolloids

journal homepage: www.elsevier.com/locate/foodhyd

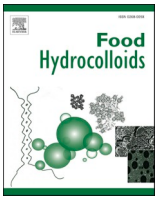

Protein-induced delubrication: How plant-based and dairy proteins affect mouthfeel

Sorin-Cristian Vlădescu [a,*], Maria Gonzalez Agurto [b], Connor Myant [c], Michael W. Boehm [d], Stefan K. Baier [d,e], Gleb E. Yakubov [f], Guy Carpenter [b], Tom Reddyhoff [a,**]

[a] Tribology Group, Department of Mechanical Engineering, Imperial College London, South Kensington, Exhibition Road, SW7 2AZ, London, United Kingdom
[b] Salivary Research Unit, Faculty of Dental, Oral and Craniofacial Sciences, King's College London, Floor 17 Guy's Tower, London, SE1 9RT, UK
[c] Robotics and Manufacturing Group, Dyson School of Design Engineering, Imperial College London, London, SW7 2AZ, United Kingdom
[d] Motif FoodWorks, 27 Drydock Ave, Boston, MA, 02210, United States
[e] School of Chemical Engineering, The University of Queensland, Brisbane, 4072, Queensland, Australia
[f] School of Biosciences, Faculty of Science, University of Nottingham, Nottingham, UK

A B S T R A C T

Understanding how certain proteins cause astringency is necessary in order to improve the mouthfeel and popularity of plant-based foods. To this end, we studied protein interactions during oral processes using a PDMS-PDMS interface lubricated by ex-vivo human saliva. Friction measurements and in-contact imaging were implemented, while food consumption was simulated by introducing model plant and animal-based proteins. All but one of the protein samples caused an increase in measured friction and this correlated with astringency ratings from a human taste panel. This is attributed to delubrication as the salivary pellicle is removed, since food proteins interact with salivary proteins thus disrupting their adhesion. This interaction is shown to occur both on the surface and in the bulk of the fluid. However, the debonding of the pellicle requires frictional shear stress (i.e., rubbing). Food proteins in isolation are themselves shown to be surface-active and form boundary films, which can adhere following removal of the pellicle. The mechanical action of protein particles in the delubrication process was isolated by filtering and shown to account for a moderate (<33%) increase in friction magnitude accompanied by a significant (>90%) increase in frictional noise. The flow and deformation of these particles was also visualised thus demonstrating how the microscale breakdown of food can be studied.

1. Introduction

By reducing meat consumption, humanity could contribute significantly to mitigating the disastrous effects of the climate crisis, lowering global CO_2 emissions by up to eight billion tonnes per year compared to business as usual (Schiermeier, 2019). However, to gain widespread acceptance, dairy and plant-based proteins must be perceived by most consumers as sufficiently appetising and palatable. Scientific studies to understand and hence control the taste and texture of dairy an[1]d plant proteins in order to increase mass appeal are therefore of paramount importance and urgency.

Recent years have seen a proliferation of research on alternative protein sources, with lower associated environmental footprints to replace meat products (Zembyla et al., 2021). These have included both proteins extracted from plants (*e.g.,* pea, soy), as well as dairy (casein, whey). However, a key challenge in assessing and enhancing the appeal of alternative proteins is determining their taste, texture and mouthfeel characteristics in a fast, reliable and cost-effective manner. Consumers' overall sensory experience is created by the organoleptic properties of foods and beverages, which contain hierarchical structures, ranging from nanoscopic to macroscopic, that determine everything from texture and nutritional value to shelf life. Rheology is an essential design tool in food engineering to improve processing, shelf stability, texture and mouthfeel, and sufficient knowledge is available on the relationship between rheology and food structures to design products with specific rheological features (Stokes and Bhandari, 2012; Stokes et al., 2013; Stokes and Frith, 2008). However, the link between these fundamental rheological properties and taste perception remains elusive (Stokes et al., 2012), nor can texture and mouthfeel be adequately anticipated through empirical techniques such as "texture profile analysis" (TPA)

Abbreviations: PID, Protein-Induced Delubrication; CoF, Coefficient of friction; PDMS, Polydimethylsiloxane; LIF, Laser Induced Fluorescence; WMS, Whole mouth saliva; DIW, Deionised water; SEM, Scanning electron microscope; IEF, Isoelectric focusing; VAS, Visual analogue scale; FPLC, Fast protein liquid chromatography; MS, Mass spectrometry; FITC, fluorescein isothiocyanate; SDS-PAGE, Sodium dodecyl sulfate–polyacrylamide gel electrophoresis.

* Corresponding author.
** Corresponding author.
E-mail addresses: s.vladescu12@imperial.ac.uk (S.-C. Vlădescu), t.reddyhoff@imperial.ac.uk (T. Reddyhoff).

https://doi.org/10.1016/j.foodhyd.2022.107975
Received 21 May 2022; Received in revised form 29 June 2022; Accepted 12 July 2022
Available online 30 July 2022

(Pons and Fiszman, 1996). For example, the mechanisms through which fat influences taste perception are insufficiently understood (Drewnowski, 1997) as is the different impact of apparently similar sweeteners on mouthfeel (Leksrisompong et al., 2012). With regard to alternative proteins, it has been demonstrated that gradually replacing milk with pea protein has a negative impact on sensorial acceptability (Omrani Khiabanian et al., 2020), but the underlying physical mechanisms remain largely unknown. These gaps in scientific understanding continue to limit rational design as a means of creating nutritious yet acceptable new food products.

Whereas sensory panels (capturing feedback from people trained to evaluate the taste, flavour and texture of food products continue to be employed to assess the appeal of engineered products (Delwiche, 2004), this approach has clear limitations including subjectivity, high cost and long duration, insufficient replicability and limited ability to capture the multidimensionality of the perceptual space over time (Labbe et al., 2009). A more reliable and scalable approach is to employ measurement techniques to understand the mouthfeel characteristics of astringency and texture perception including smoothness (Malone et al., 2003), fattiness (Malone et al., 2003), (de Wijk et al., 2006) and creaminess (Janhoj et al., 2009), (Meyer et al., 2011), the interaction of food products with saliva, the dynamic nature of oral processing and the changing status of food during consumption.

Saliva is the medium into which tastants must first dissolve and then diffuse through to reach the taste buds, most of which are located within crypts on the tongue (circumvallate and foliate papillae). Therefore, the organoleptic properties of food, including taste and texture perception, depend on the evolving status of food during oral processing alongside the changing status of the salivary film coating oral surfaces and saliva itself (Stokes et al., 2013). Since texture is a multidimensional sensory property (as reviewed by Kravchuk et al. (Kravchuk et al., 2012)) rather than a simple food property that can be measured instrumentally through imitative mechanical tests and rheology, tribological measurement techniques offer a high potential for a thorough understanding of the mechanisms impacting food acceptability. An established tribological method of assessing the change in friction following the interaction between an *ex vivo* salivary film adsorbed onto a substrate and a beverage or food sample (Bongaerts et al., 2007), (Prinz et al., 2007) has been applied to a variety of food products including tea (Rossetti et al., 2009), red wines (Brossard et al., 2016), dairy protein beverages (Vardhanabhuti et al., 2011), and custard, yogurt and cream (Selway and Stokes, 2013), as well as using different substrates (PDMS, agarose gel, pig tongue) (Carpenter et al., 2019).

One of the main challenges in the acceptance of alternative protein-rich foods is the high astringency associated with the consumption of certain proteins. Astringency, the dry sensation arising in mouthfeel perception, has been linked to a disruption of the salivary film coating during oral processing of certain molecules such as polyphenols in tea and wine (Rossetti et al., 2009). Although the perception of polyphenolic astringency was initially related to their precipitation of salivary proline-rich proteins (Humphrey and Williamson, 2001), this was challenged by studies showing the lack of PRPs in salivary film adhering to the mucosa (Gibbins et al., 2014a), (Gibbins et al., 2014b). Instead, alterations in the salivary mucins attached to the mucosal pellicle is more likely (Ployon et al., 2018) but is harder to replicate experimentally. Finally although astringency is often ascribed to the reduction in oral lubrication caused by the astringents affecting the salivary proteins, no *in vivo* evidence for such a reduction is available and some studies demonstrate a loss of lubrication is not always required for astringency to be perceived, as in the case of weakly astringent molecules (Rossetti et al., 2009), (Rudge et al., 2021).

Dairy proteins represent the primary building blocks of milk and milk-based products. In the most widely used bovine milk, the two major families of proteins are caseins and whey, found in a ratio of 4:1 (McSweeney and Fox, 2013). While whey proteins are soluble and display a compact and globular structure (Ortega-Requena and Rebouillat, 2015), casein proteins are observed as large, aggregated colloid micelles (Andoyo et al., 2014). Existing tribological studies conducted using human whole mouth saliva focused on either the mouthfeel characteristic of astringency (Biegler et al., 2016) or the contribution of fat molecules to lubrication resulting in creaminess/smoothness perception (de Wijk et al., 2006). Few studies to date have taken a comprehensive approach to investigating both the interaction of dairy proteins with salivary films or the corresponding links to mouthfeel. Fibrianto (Fibrianto, 2013) previously demonstrated that dairy proteins interact with the salivary film to increase friction but did not consider the impact of this interaction on mouthfeel attributes. More recently, Fan et al. (Fan et al., 2021) introduced a Dynamic Tribology Protocol (DTP) to assess the response of the salivary pellicle to dairy solutions and correlated their measurements to texture mouthfeel perception including thickness and smoothness. They showed that the decrease in lubricity is inversely correlated with the increase in the casein:whey protein ratio.

In contrast to the relatively simple structure of dairy proteins, pea proteins are observed as a complex set of aggregates including legumin (11 S), vicilin (7 S) and convicilin, with 11 S and 7 S subunits (Adal et al., 2017). The scientific interest in pea proteins is explained by their potential to more sustainably and cost-effectively replace whey proteins in food products due to structural similarity, since pea protein comprises of globular β-lactoglobulin (β-lg) (Sarkar et al., 2016). The main challenge related to the wider adoption of pea proteins is the associated unpleasant sensory perception associated with high reported astringency and bitter notes (Zeeb et al., 2018). However, whereas this astringency perception has been explained in the literature by the interaction of tannins in pea protein with saliva (Troszyńska et al., 2006), the physical mechanisms behind this interaction remained unknown. A recent study by Zembyla and Sarkar (Zembyla et al., 2021) analysed the surface adsorption and lubrication behaviour of both plant and animal proteins on mucin-coated substrates. This revealed that, at increased concentrations (100 mg/mL), whey protein provides superior lubricity compared with pea protein, while at lower protein concentration (<10 mg/mL), the whey protein isolate was less lubricious compared with extensively hydrated mass of pea protein isolate.

The current study uses a range of experimental techniques to probe a biomimetic sliding saliva-lubricated oral interface during the simulated consumption of both dairy and plant proteins in order to understand the lubrication breakdown mechanisms under closer to real-life conditions. In addition to the insights gained, this approach paves the way toward rapid and cost-effective means of testing novel food products and thus reducing the food industry's reliance on lengthy and subjective panel testing and hence accelerating rational food design processes.

To reveal underlying mechanisms under biomimetic conditions, different proteins are tested under two distinct scenarios: (1) *in vitro* oral mimicking setup using freshly collected human whole saliva adsorbed onto a soft PDMS mimicking the oral mucosa and (2) *in vitro* oral mimicking setup using a biological (porcine) tongue to accurately mimic oral surfaces in terms of elastic modulus, roughness and surface energy. The main advantage of the first setup consists in the addition of a LIF microscopy technique to detect labelled proteins at the contact zone between the sliding surfaces. This approach also facilitates the understanding of the dynamic behaviour of dairy and plant proteins, their changing status during oral processing, as well as the underlying physics/mechanics that ultimately account for mouthfeel perceptions. The second setup is employed as a means of assessing the accuracy of astringency measurements in the context of real tongue tissue. For further validation friction measurement are compared to astringency ratings from a human taste panel.

2. Materials and methods

2.1. Description of experimental apparatus

Two setups were used to assess the response of the salivary pellicle (using freshly collected whole human saliva) to the addition of plant-based and dairy protein under lubrication conditions that closely mimic those found within the oral cavity:

i) a rotating configuration where a 12.5 mm radius poly-dimethylsiloxane (PDMS) hemisphere was loaded against a PDMS substrate fixed on a glass disc (Fig. 1a) and operated in pin-on-disc mode, with the PDMS disc rotating against the stationary silica hemisphere. The added benefit of the PDMS substrate is its optical translucency permitting microscopy at the contact zone. Combined with a fluorescence detection, this allows labelled salivary (Vlădescu et al., 2021) or food proteins to be viewed in the contact. Previously, we have shown that PDMS accurately mimics tongue tissue and confirmed the excellent lubricating properties of saliva (100 times better than pure water) (Carpenter et al., 2019), (Vlădescu et al., 2021). The PDMS specimens were moulded using a commercially available Dow-Corning Sylgard 184 kit, containing a base and curing agent to produce a substrate with a Young's modulus 1.84 MPa at 23 °C.

ii) a reciprocating configuration, where the same PDMS hemisphere was loaded against a porcine tongue (Fig. 1b), the latter being fixed on a reciprocating table and slid against the stationary silica hemisphere over a 24 mm stroke distance. The porcine tongue, procured and tested on the same day, had its underside removed to produce a slab of even thickness. This specimen was then attached to a flat plate using cyanoacrylate adhesive and mounted in the reciprocating drive of the tribometer.

The two configurations were successively installed on a UMT-2 tribometer (Universal Materials Tester from Bruker), which permits sliding speeds of 0.5–20 mm/s, as encountered in the tongue-palate contact (Hiiemae and Palmer, 2003), while simultaneously adjusting and measuring normal load and friction force via strain gauges attached to the housing over the silica specimen. The purpose of the two set-ups is fundamentally different:

(1) The rotating, transparent setup facilitated the visualisation of salivary film-proteins' interactions using a custom-built, Laser Induced Fluorescence (LIF) microscope mounted beneath the supported transparent PDMS and focusing on the sliding contact. Here, incident light from the microscope's blue (490 nm) LED excited dyed proteins at the interface, resulting in fluorescence. As incident and emitted light are of different wavelengths, they could be separated by a dichroic filter (25 mm × 36 mm long-pass, 567 nm cut-on), with the resulting images captured by a high-speed, intensified camera (Phantom Miro eX4). These images depicted the varying thickness of dyed proteins around the contact, since for film thicknesses greater than 200 nm, the intensity of emitted fluorescence light correlates with the thickness of the pellicle. The microscope objective used in this study was a Mitutoyo Plan Apo with a 2X magnification, 0.055 numerical aperture, and a 91 μm depth of field, while the selected optical lens was an achromatic doublet AR coated for the 400–700 nm range. A detailed description of the LIF technique can be found in (Carpenter et al., 2019), (Vlădescu et al., 2021), (Vladescu et al., 2018).

(2) The reciprocating, porcine tongue setup allowed a comparison of protein samples under more realistic oral mucosa conditions (*i.e.,* stiffness, surface roughness) in order to validate the measurement and observation obtained using the pin-on-disc configuration. The porcine tongue was fixed in the reciprocating tribometer in Fig. 1 (image insert), using a procedure described in (Carpenter et al., 2019) and tested on day of purchase.

2.2. Sample preparation

Five plant-based and dairy protein samples were sourced, their typical composition and nutritional values being detailed in Table 1. The two pea proteins, P870 and Pulse 1803, were produced by PURIS™ and Ingredion Incorporated, respectively. The whey proteins, Hilmar 9000 and Hilmar 9400 were both produced by Hilmar Ingredients™, while the Micellar Casein was produced by AMCO Proteins.

For friction measurement tests, samples were prepared 1h prior to each PID tasting session. Using a high-accuracy scale, 1.00 g of protein was mixed with 30 mL of deionised water (DIW) using a rotary lab shaker for 3 min and then stored at constant room temperature (25 °C) for 1 h. This was repeated for all five protein samples.

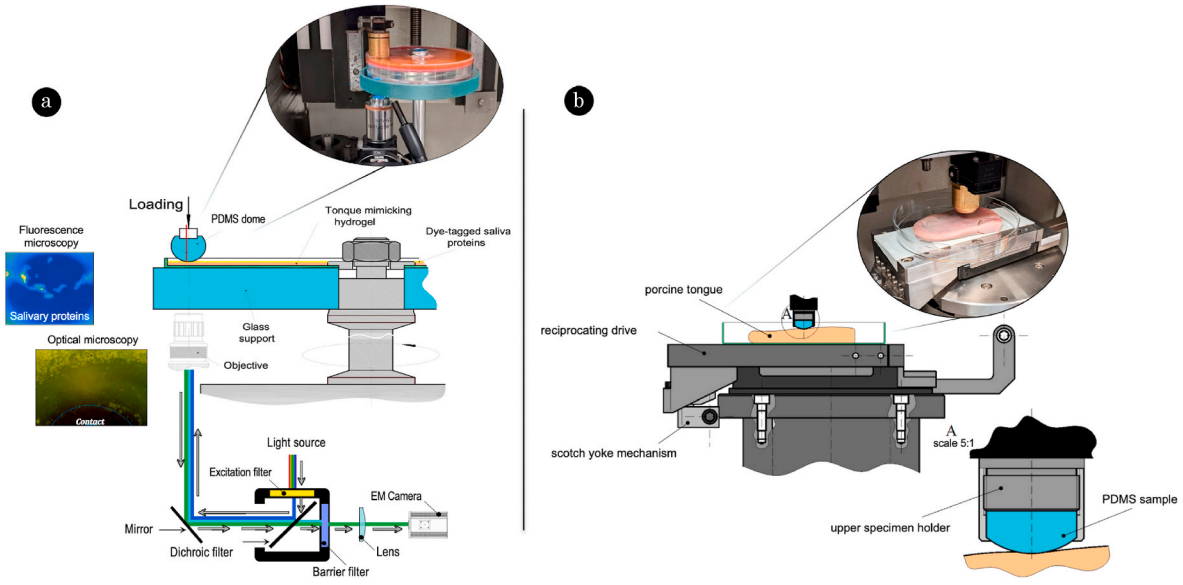

Fig. 1. – a) Schematic representation of the rotating, transparent oral mimic visualisation setup (Insert: photograph of laser induced fluorescence microscope setup); b) Schematic representation of the reciprocating setup (Insert: photograph of modified PDMS-on-porcine tongue CETR UMT2 tribometer).

Table 1
Typical composition and nutritional values of the five plant-based and dairy proteins employed in this study.

	Sample Name				
	PURIS™ P870	VITESSENCE™ Pulse 1803	AMCO Micellar Casein	HILMAR™ 9000	HILMAR™ 9400
Image/Colour	 Cream, Off White	 Cream, Off White	 White	Cream	 Cream
Protein Type	**PEA**	**PEA**	**CASEIN**	**WHEY**	**WHEY**
Protein Concentration [% dry basis]	Min. 80	Min. 80	Min. 85	93	93.4
Moisture [g/100g]	Max. 6	Max. 10	Max. 6	Max. 5.5	Max. 5.5
Fat [g/100g]	6.0	7.8	Max. 2	Max. 1	Max. 1
pH	6.5–7.5	7.0–8.0	6.4–7.0	6.1–7.0	6.2–7.0
Ash [%]	5	4.7	7	2.5	2.6
Sodium [mg/100g]	750	1170	100	155	835
Potassium [mg/100g]	200	92	250	545	110
Calcium [mg/100g]	400	91	2300	425	110

Next, to visualise protein motion, size and distribution in and around the contact, the samples were doped with a fluorescent dye, Sulforhodamine G (0.05% mass concentration). To achieve the latter, the image of a precision graticule was captured while positioned on the PDMS disc, which allowed for a conversion of number of pixels to millimetres (see Supplementary Materials).

2.3. Saliva collection

Whole mouth saliva (WMS) was collected from a single male (37 yrs) donor, to ensure consistency, as previously reported in (Carpenter et al., 2019), (Vlădescu et al., 2021). The donor refrained from ingesting any products, except pure water, for at least 120 min prior to collection and then swilled water around the mouth for at least 30 s. The saliva expectorated during the first 60 s was eliminated, prior to collecting the final test sample into a glass tube and stored on ice. To remove sloughed cells and other impurities, the sample was centrifuged for 3 min (1000 g).

Following centrifugation, the collected saliva was immediately employed in a PID tribological measurement. This was important as a preliminary test showed that the friction characteristics and thus the lubricating properties of fresh saliva degrade within 15 min after the time of collection.

2.4. Protein-induced delubrication (PID) tribological protocol

The tribological protocol used here to assess food protein induced delubrication (PID) of the pre-adsorbed salivary pellicle was adapted from studies by Stokes et al. (Rossetti et al., 2009), (Fan et al., 2021). Each transient, time-dependent frictional response was recorded at room temperature (25 °C), using a constant sliding speed for both rotational and reciprocating setups, of 3.1 mm/s and 4.6 mm/s respectively. In both scenarios, the PDMS hemisphere was pressed against the PDMS disc or porcine tongue using a load of 0.5 N. Three repetitions were performed per protein sample, each composed of the following sequential steps:

1. Dry friction was measured for 60 s.
2. 1.5 mL of WMS was gradually added on the PDMS disc, in front of the contact, using a pipette. This ensured that a thin saliva pellicle would form and adsorb evenly onto the disc, along the path of the point contact. The frictional response generated by the salivary pellicle was continuously recorded for 10 min, using a sampling rate of 200 Hz.
3. While continuing the sliding motion and maintaining the applied load, the protein solution mix (1 g of protein mixed into 30 mL of deionised water) was carefully added on top of the saliva, completely covering the already formed salivary track. Friction data points were continuously recorded for another 30 min at the same sampling rate of 200 Hz.

Before each test, the PDMS surfaces were cleaned with isopropanol and deionised water by sonication, each for 10 min. Before each test session, the PDMS surfaces were subject to a run-in process consisting of 5 min of dry friction, followed by 20 min of sliding under deionised water lubricated conditions. We devised a strict set of assessment criteria to qualify each PDMS tribopair for testing and thus avoid sources of variability. The two conditions which had to be met simultaneously were: *i)* a 'dry' friction coefficient between the PDMS substrates in the range of 1.25–1.45, and *ii)* a DIW friction coefficient of the PDMS tribopair in the range of 1.05–1.2.

2.5. Human taste panel testing

A series of Visual Analogue Scale (VAS) sensory assessments were completed (approved by the Research Ethics Office (HR/DP-20/21–23121)). The sensory panel consisted of ten experienced subjects (4 male, 6 female), formally recruited and trained for sensory evaluation studies. Subjects were asked to taste the three samples (deionised water, pea 1803 and pea P870 solutions) at random and provide VAS scores for each one. The two pea protein solutions were prepared with an identical concentration as described in Section 2.2 (*i.e.,* 1.00 g of protein mixed with 30 mL of deionised water).

3. Results and discussion

3.1. Particle size measurements, staining results and ionic analysis

The protein concentration of the five plant-based and dairy proteins was determined using the BCA Protein Assay Kit (Thermo Fisher Scientific, IL, USA). Pea P870 (3.39 μg/μl) and pea 1803 (4.18 μg/μl) showed similar values, however casein (8.1 μg/μl), whey 9000 (9.75 μg/μl) and whey 9400 (9.85 μg/μl) were almost twice as high as those recorded for both pea proteins.

The size and shape of the protein particle samples were determined using scanning electron microscopy (SEM) under dry conditions, as well as after their dispersal in deionised water.

SEM analysis of the dry proteins (Fig. 3(a)) showed larger particles for pea 1803 and an increased amassment of smaller particles around the large ones. Further inspection of the SEM scans showed larger size particles for pea 1803 compared to pea P870 (in the range of 10–200 μm for 1803, versus 5–80 μm for P870). Following a 1 h rest in deionised

water, the aggregated pea 1803 proteins exhibited a viscous look, although the shape of the pea particles remained visible (Fig. 3(b)).

SEM images of both whey 9000 and 9400 showed hollow, sphere-shaped particles, with smoother, more brittle structures observed for the former. Following the addition of dispersant, the measured whey particles were in the range of 20–200 nm, which agreed with data reported by Jambrak et al. (Jambrak et al., 2014).

Isoelectric focusing (IEF) technique (Fig. 2(c)), which separates proteins according to their isoelectric point (no net charge) indicated most bands were between pH 4.5 to 6 for the five samples. This contrasted with their pH when dissolved in water (mostly between 6 and 7) which suggests most proteins will have a negative charge.

Furthermore, despite SDS PAGE (Fig. 2(d)) indicating both pea preparations having the same proteins (assessed by apparent molecular weight) in similar quantities, the chromatographic (FPLC) data showed in Fig. 2(e) highlights a clear difference between the two pea samples. More precisely, pea P870 presented larger peaks eluting earlier which indicates high molecular weight aggregations of proteins, whereas pea 1803 proteins eluted later. This variation in molecular weight observed for two pea solutions can be attributed to the superior binding properties of pea P870.

Finally, the composition of the two pea proteins was assessed using mass spectrometry (MS)-based proteomics of trypsinized peptides. Although the proteomics heat map (Fig. 2(f)) showed a similarity in

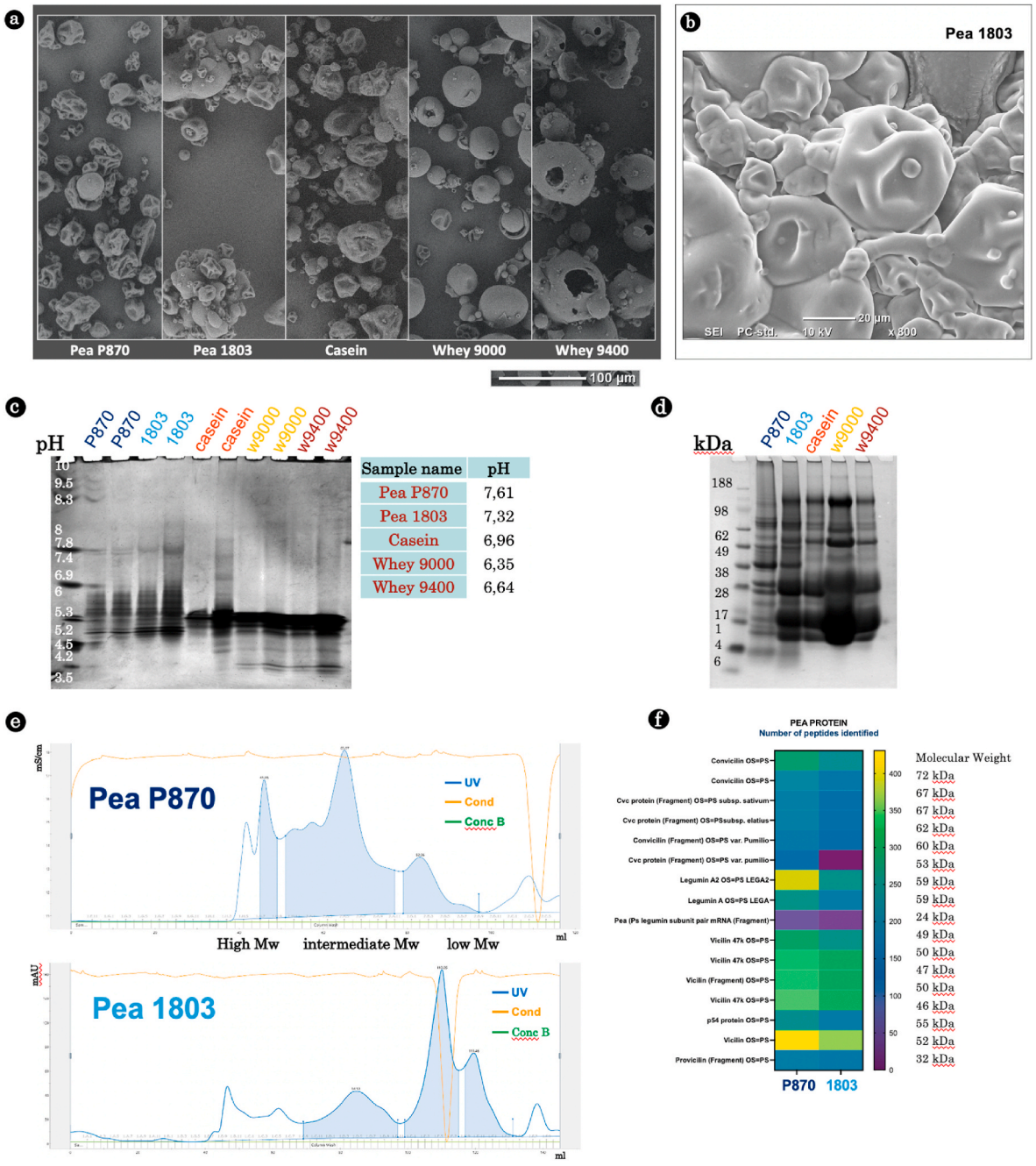

Fig. 2. – Characterization of the five (plant and dairy) proteins: a) Scanning electron micrographs of the five astringent samples recorded prior to their addition into DIW dispersant; b) SEM scan of the pea 1803 sample following 1 h rest in DIW; c) SDS-PAGE CBB R250 stained food proteins allowing their separation by mass; d) Isoelectric focusing (IEF) of all five proteins e) Fast protein liquid chromatography of the two pea proteins; f) proteomic mass spectroscopy of the two pea proteins preparations.

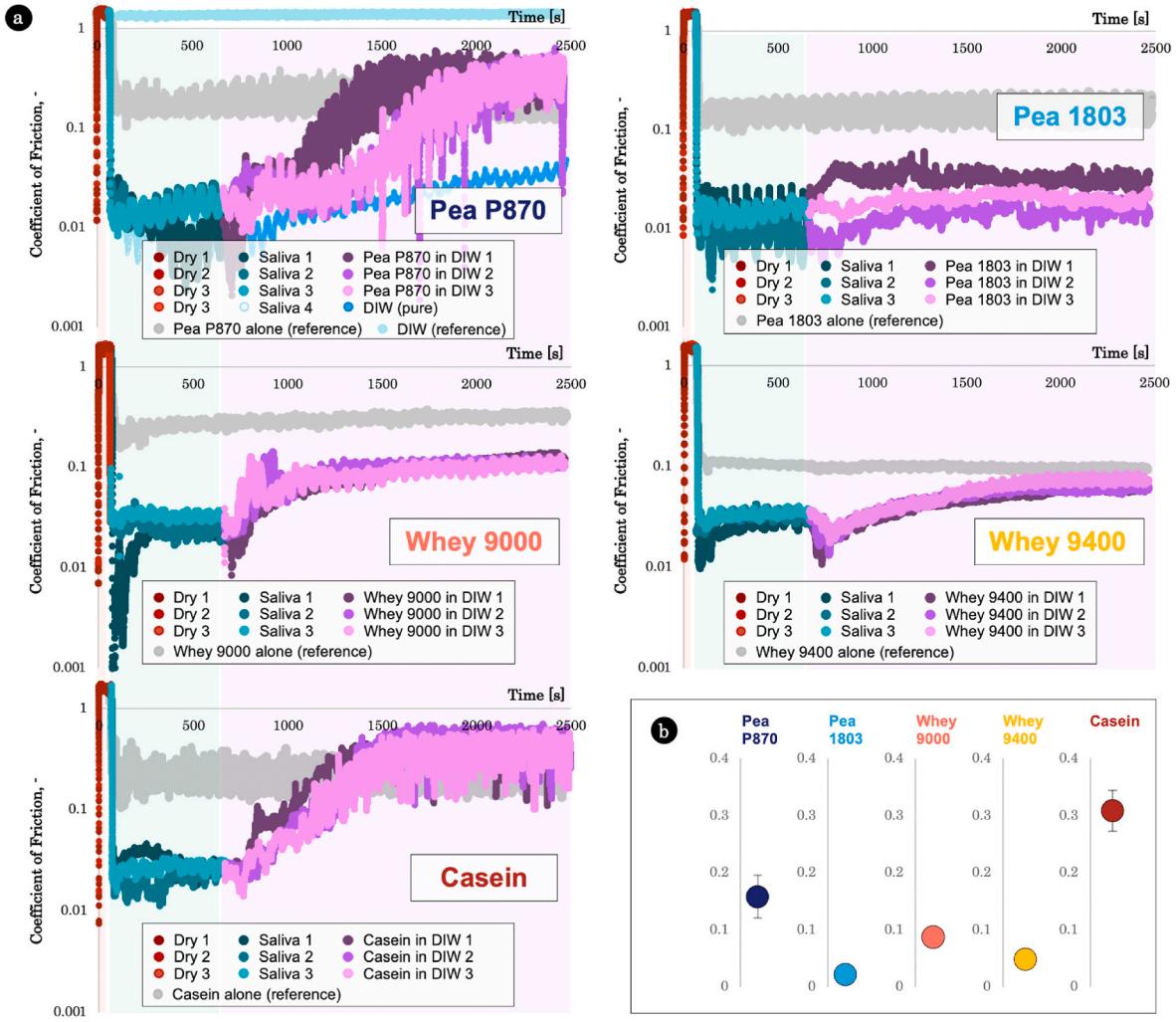

Fig. 3. (a) Comparison of friction coefficients measured for all five proteins. Repeatability between three different tests is highlighted for each sample. Each PID test protocol comprises three consecutive steps, highlighted above using three distinct colours: Step 1 (t = 0–60 s, brown font) – Dry friction; Step 2 (t = 61–660 s, green font) – Addition of saliva; Step 3 (t = 661–2461 s, purple font) – Friction coefficient variation after the addition of proteins; (b) Average values (± SD) across all three Step 3 repetitions shown in Fig. 3(a) above. (For interpretation of the references to colour in this figure legend, the reader is referred to the Web version of this article.)

protein conformation for both pea proteins, it also revealed differences in the number of peptides in pea P870 and pea 1803.

3.2. Friction results (protein-induced delubrication)

The friction response of the protein samples was assessed using the protocol described in Section 2.4: (1) dry sliding for 60 s, 2) addition of saliva followed by 600 s sliding to form pellicle, 3) addition of astringent sample followed by 30 min recording of friction response). To assess repeatability, all tests were repeated three times on non-consecutive days.

Fig. 3 shows greater friction increase after adding pea P870 and casein, with both samples acting to rapidly increase friction that reaches approximately 0.38. Contrastingly, pea 1803 and the two whey samples show coefficients of friction remaining below 0.1. This may indicate that these latter samples have reduced impact on the salivary pellicle, which maintained lubricating even after 30 min of sliding. And in fact, none of the friction trends following PID approach that of pure water (shown for reference in the pea P870 plot) suggesting a protein film always remains. However, it should be noted that all the tested food proteins are themselves surface-active since they provide low friction when tested without saliva (grey lines). Furthermore, following delubrication, the friction in the PID tests for pea P870, whey 9400 and casein tend towards the same value as that of the food protein-adhered film. Therefore, apparently milder delubrication is likely to result not from limited removal of the saliva pellicle but rather it being either replaced or covered by somewhat lubricious plant-based proteins.

The response for all samples, and most clearly whey 9400, include an initial reduction in friction immediately after they are entrained, which may be due to astringent proteins interacting with saliva proteins accumulated at the inlet. This could cause the observed reduction in friction if the accumulated proteins at the inlet were to detach from the surfaces and become entrained through the contact (we have previously observed similar transient friction reductions due to entrainment of saliva agglomerations (Vlădescu et al., 2021)). Moreover, protein agglomerations trapped at the inlet can act to feed the contact and provide additional lubrication (*e.g. Inlet-Protein-Agglomeration* mechanism as observed in contacts lubricated by synovial fluids (Fan et al., 2011)), therefore, removal of this mechanism would subsequently result in an increase in friction as indeed is shown in Fig. 3. This inlet delubrication mechanism seems to occur more rapidly for whey 9000 than for 9400 which may be due to the specific interaction with salivary proteins at the contact inlet (the former appears to disperse the proteins around the inlet while the latter causes them to be entrained through the contact).

This inlet delubrication mechanism is later visualised using fluorescence in Section 3.4.

To rank the delubrication capabilities of the five proteins, all friction data points recorded during Step 3 (*i.e.,* 660–2460 s) were averaged across all three repetitions and plotted in Fig. 3(b).

To further validate the protein induced delubrication behaviour observed in the PDMS-PDMS, contact (Fig. 1(a)), pea P870, pea 1803, and the casein proteins, were tested in the real porcine tongue setup shown in Fig. 1(b) using a similar protocol as above. As shown in Fig. 4 (graphical detail), the frictional response of pea P870 is approximately double in magnitude when compared with that of pea 1803, with casein again giving the highest friction. For all three protein samples, there is very good agreement between the frictional response measured in the reciprocating, real tongue test and the PDMS-PDMS test (Fig. 3).

The question arises as to what generates the observed differences in frictional response between samples. For instance, the enhanced delubrication could be generated by: *i)* a bulk change in viscosity of the solution vs. adhered surface film removal, or *ii)* a reaction between saliva and astringent proteins vs. mechanical astringent particles, either due to abrasive wear as they are entrained through the contact or by causing starvation as they accumulate in the inlet. To shed light on the PID mechanisms, friction was measured as a function of speed (to obtain Stribeck curves) thus varying the lubrication regime. Stribeck curves often show friction versus the product of speed and fluid viscosity (de Vicente et al., 2006). However, saliva is highly non-Newtonian and its viscosity varies due to both its inhomogeneous composition and its dependence on shear rate (Carpenter et al., 2019). Thus, Stribeck curves shown here vary just sliding speed alone (between 0.6 and 18.8 mm/s, a range typically encountered in oral food processing).

In addition to the friction test results shown in Fig. 4(a), a series of Visual Analogue Scale (VAS) sensory assessments are shown in Fig. 4(b). The strong PID – Astringency corelation observed in Fig. 4 for the two pea proteins supports the hypothesis that pronounced salivary delubrication (due to food proteins interacting with salivary proteins and disrupting their adhesion) is directly responsible for an increase in perceived astringency.

Fig. 5 shows seven consecutive Stribeck curves for pea P870, under two different scenarios: *i)* protein solution mixed beforehand with the 1.5 mL of WMS, then added on the PDMS disc (Fig. 5(a), and *ii)* protein solution added on top of an already established salivary film, formed on the PDMS surface (Figs. 5(b) −1.5 mL of WMS were added on the PDMS disc and rubbed against the counterpart PDMS dome for 10 min prior to the addition of the protein solution). Both plots show friction reducing with increasing speed as more fluid is entrained and generates a greater hydrodynamic pressure that acts to separate the surfaces and reduce adhesion.

Fig. 5(a) shows an initial friction coefficient of ~0.1 for Test 1, followed by a rapid increase (tests 1 to 2) and then a gradual increase (tests 2 to 7). This suggests that the pea/saliva interaction occurs in the bulk of the fluid prior to the sliding test so that the resulting denatured saliva proteins adhere only weakly to the PDMS surface and are therefore immediately removed during sliding. Alternatively, the poor lubrication when the mixture is added directly, may be due to the pea proteins competing and preferentially adsorbing on the PDMS surfaces. Contrastingly, Fig. 5(b) shows a gradual increase in friction when the astringent is added to the previously formed saliva film. These

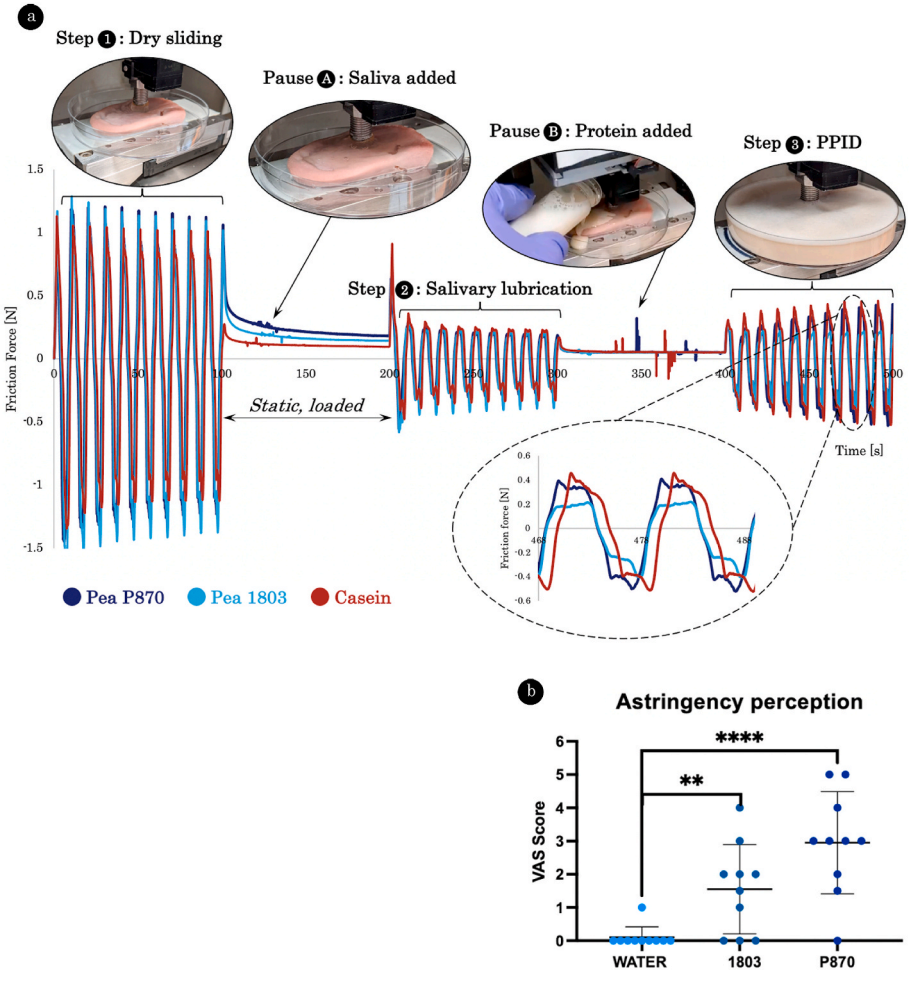

Fig. 4. (a) Friction force variation for Pea P870 and Pea 1803, and casein. Step 1 – frictional response along 20 strokes under dry lubrication conditions; Pause A – Addition of saliva during a 100 s resting period (static, loaded contact); Step 2 – friction behaviour of the salivary lubricated porcine tongue - PDMS hemisphere contact; Pause B – Addition of protein on top of the salivary film during a second resting period; Step 3 – PID as recorded for each of the plant-based and dairy proteins. For each of these steps, friction was recorded for 100 s (20 strokes), while maintaining the applied load (0.5 N) and sliding speed (4.6 mm/s). The reciprocating motion was paused after each step - the two pauses of similar duration allowing for the addition of the WMS (Pause A) and the protein solutions (Pause B) on top of the tongue sample; (b) VAS score of 10 subjects ($p < 0.0001$ **** (Pea P870/DIW), $p < 0,0038$ ** (Pea 1803/DIW), $p < 0.0436$ * (Pea P870/Pea 1803)).

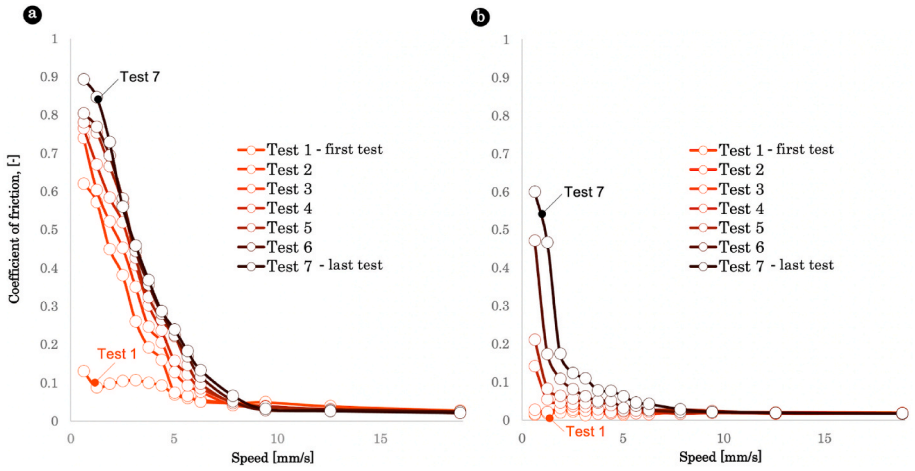

Fig. 5. Speed-dependent Stribeck curves highlighting for two scenarios *a)* human collected saliva mixed directly with pea P870 solution before being poured onto the PDMS surface, *b)* a salivary layer was adsorbed on the surface and rubbed for 10 min prior to the addition of pea P870.

observations support the idea that astringency can result from both surface and bulk interactions. It is also interesting that the interaction in the bulk of the fluid (Fig. 5) results in an increase in friction that is both faster and more severe. Finally, all tests in Fig. 5 show friction measurements above 8 mm/s to be constant and at a similar level to pure saliva. This suggests that the lubrication breakdown is due to surface (boundary) film prevention/removal rather than a reduction in bulk viscosity, since under these higher speed conditions the entrained fluid is completely separating the surfaces (full-film hydrodynamic regime). Moreover, delubrication is unlikely to have been caused by food proteins starving the contact inlet (as occurs when gas bubbles in carbonated water is entrained (Vlădescu et al., 2021)), since the latter would not increase boundary friction at low speed.

Stribeck curve repetitions for the other test samples exhibit similar characterises to those of pea P870 and are shown in Supporting Information.

3.3. Particle distribution and their effect on the delubrication process

Fig. 6(a) shows the friction response for the pea and casein proteins for both filtered (using a Corning® 0.2 μm filter) and unfiltered solution. Although the general delubrication trends are unaffected, the unfiltered samples show a much noisier frictional response. Filtration increases average friction (averaged from 660 to 2460 s and shown in Fig. 6(b)) by 30% and 33% for pea P870 and casein, respectively. This moderate change in magnitude is accompanied by significant particle induced noise that is likely to affect mouthfeel. To isolate the friction noise caused by the dispersed insoluble particles in the unfiltered protein

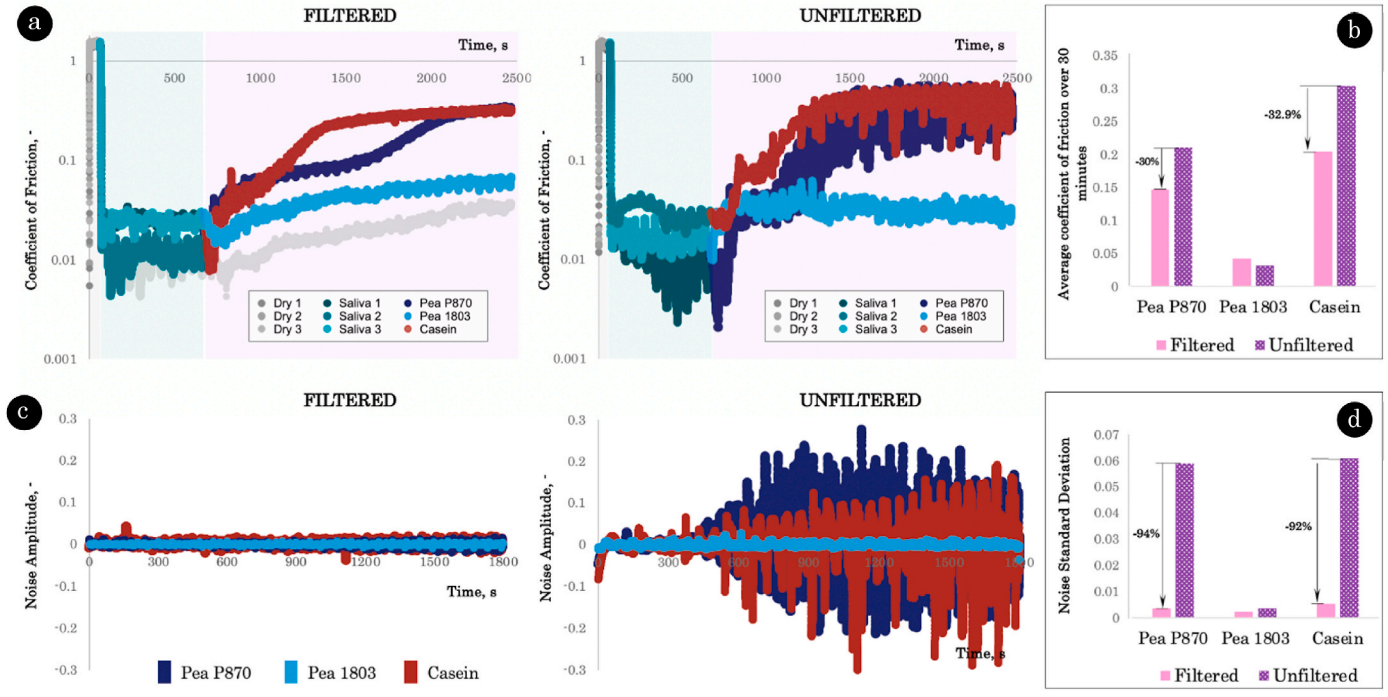

Fig. 6. (a) friction coefficient comparisons from PID tests under two scenarios: protein solutions filtered using a Corning® 0.2 μm filter versus unfiltered protein solutions; (b) averages of coefficient of friction data recorded from the moment the protein solutions were added on to the adsorbed salivary layer (seconds 660 to 2460); (c) Noise amplitude generated by both the filtered and unfiltered protein solutions; (d) Standard deviation of the noise amplitude shown in Fig. 6(c) plotted for all three protein solutions under both filtered and unfiltered tests.

solutions, Fig. 6(c) plots the friction after a smooth polynomial function was subtracted from the original data. Fig. 6(d) then quantifies the noise amplitude by the standard deviation of data in Fig. 6(c). This shows that filtering P870 and casein to remove particles, reduces friction noise amplitude of >90%.

3.4. Fluorescence results

To understand the protein-induced friction increase, in situ Laser Induced Fluorescence (LIF) imaging was applied alongside the friction measurements. For films thicker than 200 nm, fluorescence intensity is proportional to thickness (*i.e.,* the thicker the lubricating film, the higher the light intensity) (Myant et al., 2010; Vladescu et al., 2016; Vlădescu, 2016; Vlădescu et al., 2017). Therefore, the recorded intensity gives an indication of the salivary pellicle thickness. Here, salivary proteins were tagged with fluorescein isothiocyanate (FITC) and P870 was added on to the formed pellicle. Fig. 7 (a) shows the resulting friction increase, while (b) shows the fluorescence intensity (a proxy for pellicle thickness) averaged in two regions: (i) at the inlet upstream of the contact, (ii) within the contact (regions shown in (c)). As the astringent sample is added (around 520 s), there is an immediate drop in friction coinciding with a decrease in fluorescence intensity in the inlet and increase within the contact. This suggests that lubricious salivary proteins previously trapped in the inlet are dislodged and become entrained temporarily reducing the frictional response (1&2 in Fig. 7(d)). This is followed by a gradual decrease in fluorescence intensity, both at the inlet and within the contact, suggesting that a gradual debonding of the salivary pellicle is responsible for the concurrent steady increase in friction.

To study the transient mechanisms responsible for the increased friction caused by the unfiltered pea and casein protein solutions, the delubrication process in Fig. 3 was viewed using laser induced fluorescence microscopy. In these tests, Sulforhodamine G dye was used to tag the food protein particles and salivary proteins adhered to the PDMS surfaces.

Fluorescent images were obtained for the two pea and casein proteins at two instances during the delubrication process (Fig. 8(a)): *i)* Step 1, 150 s after the addition of the protein solution on top of the salivary layer (*i.e.,* second 670), and *ii)* Step 2, at the end of the test, 1800 s after protein solution entrainment.

Fig. 8(b) shows the average in-contact fluorescent intensity, indicating saliva pellicle thickness. For all three samples, the intensity at Step 2 is less than at Step 1, demonstrating that the observed increase in friction over time (Fig. 6) is caused by a reduction in in-contact thickness of the salivary film. Also, the ranking of increasing fluorescence intensities between samples (pea 1803 > pea P870 > casein (Fig. 8(b)), is the reverse of the ranking of increasing friction (casein > pea P870 > pea 1803, Fig. 6). This shows that the greater the ability of a food protein to remove the salivary pellicle from within the contact, the more pronounced the delubrication behaviour. Both the above observations are summarised in Fig. 8(c), which plots the average in contact intensity (∝ film thickness) vs. the corresponding friction for all three samples and both time steps. This suggests that, following delubrication by pea P870, whey 9400 and casein, the observed trend in friction value towards that of the neat astringent (Fig. 3) is not due to a covering over of the salivary pellicle, but rather the pellicle being removed and followed by adsorption of the astringent on the surfaces.

Fig. 8(a) also elucidates particle behaviour. At Step 1, food proteins become trapped and agglomerate in front of the contact inlet. But some P870 particles, having the small diameter (~5–80 μm *vs.* 10–200 μm 1803 and 5–180 μm casein), are entrained into the inlet, causing high amplitude frictional noise observed in Fig. 6. Over time (Step 2), due to mechanical shearing and/or softening, particles encroach further into the contact (accompanied by an increase in area as gap thickness reduces). For pea P870 and casein, this increases frictional noise (Fig. 6). However, for pea 1803 a particle-free zone remains in front of the contact where the gap height is too thin to admit food protein particles, which explains the negligible frictional noise for this sample (Fig. 6).

In situ LIF images reveal a range of particle transport mechanisms as highlighted by the dye-tagged casein example in Fig. 9 and video 1. Upstream of the contact, particles which are smaller than the gap height between specimens travel with the same velocity as the surrounding fluid (A), whereas particles within the contact become trapped (B). Near the contact inlet, particles turn back due to the re-circuiting flow caused by the narrowing gap height (C). Finally, due to the shearing action of the contact, agglomerated particles are broken down into single particles and entrained through the contact (D), causing the friction noise observed in Fig. 3. Once entrained inside the contact, particles/clusters simultaneously increase in lateral size and reduce in intensity (*i.e.*, vertical thickness) as shown by (Fig. 10).

Supplementary video related to this article can be found at https://doi.org/10.1016/j.foodhyd.2022.107975

Next, particle deformation is studied. Fig. 10(a) shows a LIF image of a dyed pea 1803 particle located close to the contact inlet, while Fig. 10 (b) shows the deformed contact geometry calculated from Hertz theory

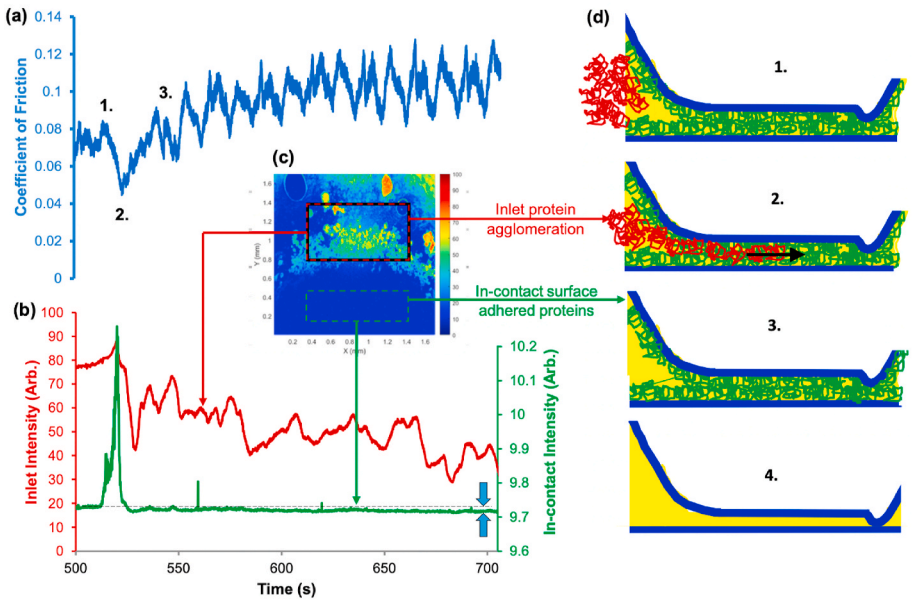

Fig. 7. Pea P870 protein-induced delubrication process of a FITC-tagged salivary film; a) Coefficient of friction, c) Varying average fluorescence intensity of dye-tagged saliva proteins – red line shows average intensity at contact inlet, green line shows average intensity within contact, c) Fluorescent image of the contact, d) delubrication process: 1. Proteins adhered to surfaces (green) and agglomerated at the inlet, 2. Astringent added causing agglomerated contact to become entrained, 3–4. Gradual debonding of in-contact salivary pellicle. (test conditions: applied load – 0.5 N, sliding speed – 3.1 mm/s). (For interpretation of the references to colour in this figure legend, the reader is referred to the Web version of this article.)

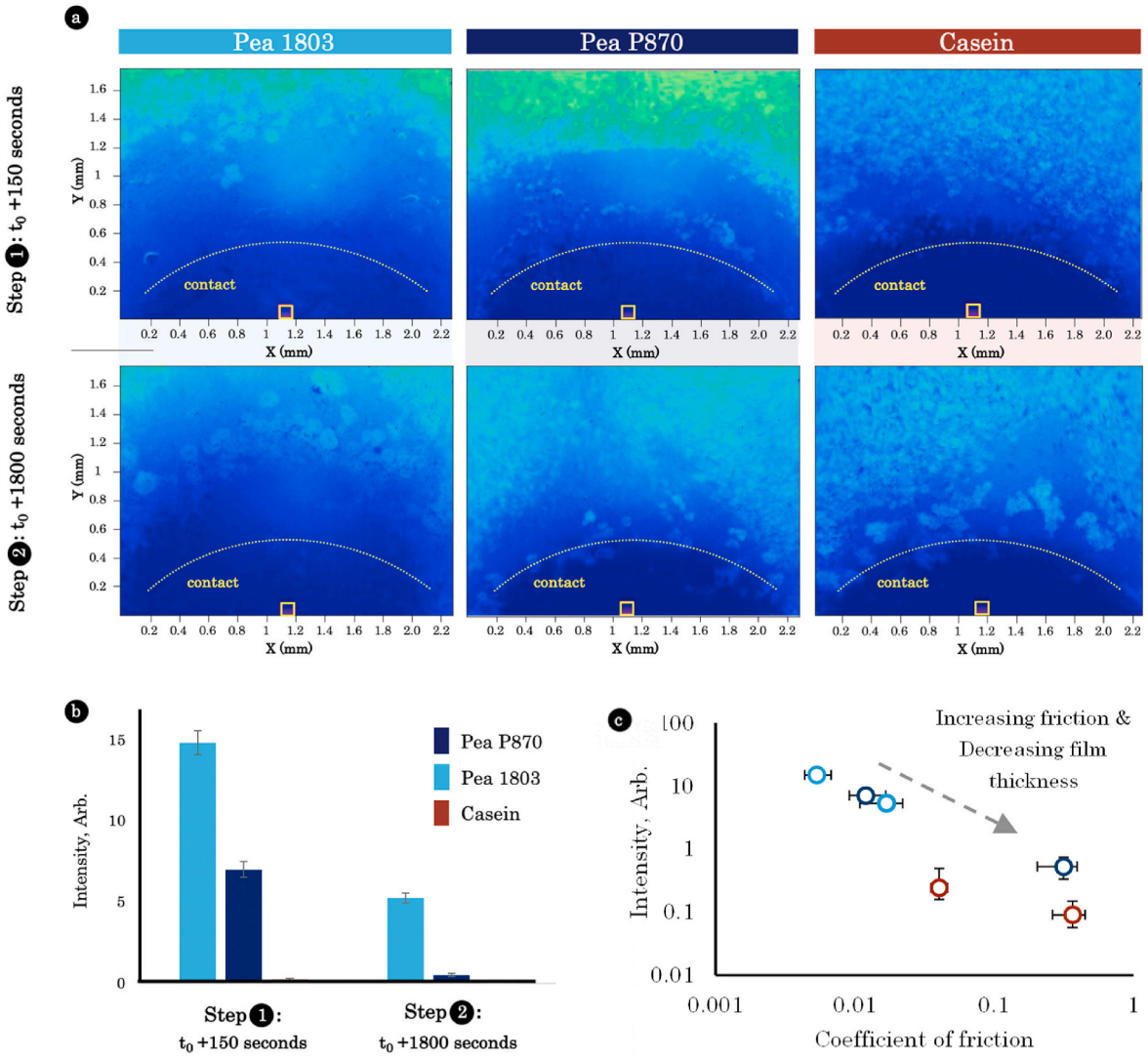

Fig. 8. (a) – Video frames from the LIF microscope (obtained during: Step 1 – t0 + 150 s after addition of proteins; Step 2 – t0 + 1800 s after) for both pea proteins (P870 and 1803), and casein. Sliding speed fixed at 3.14 mm/s, applied normal load: 0.5 N. The contact area is highlighted by the yellow dotted arc. (b) In-contact fluorescence intensity averaged from the 20 × 20 pixel areas highlighted in (a) over a sequence of 50 frames; (c) average in contact intensity (∝ film thickness) vs. friction for all three samples and both time steps. (For interpretation of the references to colour in this figure legend, the reader is referred to the Web version of this article.)

following (Vlădescu et al., 2021), from which the particle height can be estimated Fig. 10(c). Compared to an initial diameter of ~85 μm, this shows how protein particles become deformed due to the motion of the contact, (in this case extruded/sheared into a 180 μm diameter disc). This particle breakdown process is linked to the frictional response, since the forces required to deform particles give rise to the frictional noise that is measured and isolated in Fig. 6. Moreover, these interactions are important as they are likely to affect mouthfeel.

This is a demonstrative example, in which an arbitrary single particle has been selected in order to show the potential of this approach. From here, the approach can be expanded to follow the deformation of populations of particles and used to compare how readily different proteins break down as they are consumed. Moreover, using approaches such as in-contact infrared microscopy, deformation processes (shearing vs. extrusion) can be distinguished viewed in greater details (as has been demonstrated for bearing particles (Reddyhoff et al., 2018).

4. Conclusions

We used tribological measurements combined with in-contact fluorescence imaging to study the breakdown of the salivary pellicle by food proteins within a simulated tongue-palate interface. The measured friction increase resulting from the introduction of food protein onto a saliva film on PDMS agreed with that from a biological tongue and correlated with astringency ratings from a human taste panel. This confirms that astringency is a lubrication breakdown process and demonstrates how it can be characterised ex-vivo using an oral mimic which may be more rapid, reliable, and quantitative than conventional taste panel testing. The following picture is revealed:

Both plant-based and dairy proteins can cause astringency by interacting with saliva proteins thus reducing their adhesion to the surface. This interaction can involve saliva proteins bound to the surface (*i.e.,* the pellicle) and also those within the bulk of the fluid. Following this interaction, shear stress is required to remove the weakly bound saliva proteins to cause delubrication. Changes in bulk hydrodynamic/viscous friction due to saliva-astringent interactions were negligible compared to this surface effect.

A second mechanism is that, during the formation of the salivary pellicle, salivary proteins agglomerations are trapped at the inlet and act to feed the contact, providing additional lubrication (the *Inlet-Protein-*

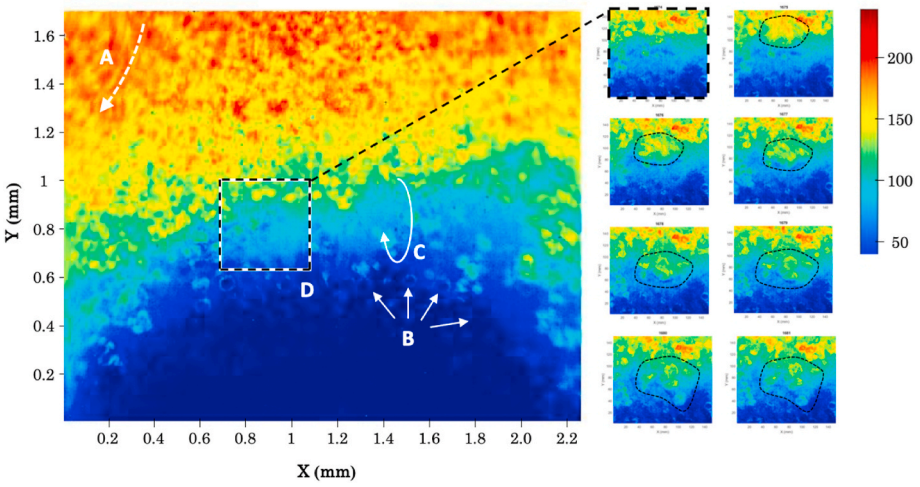

Fig. 9. Fluorescence image of contact after the introduction of dyed casein. Also see video in supplementary information. A) Particles located away from the contact are travelling with bulk fluid velocity, B) Particles within the contact become trapped/stationary, C) Recirculation of particles, D) Agglomerated particles are broken down as they are entrained through the contact (particles/clusters simultaneously increase in lateral size and reduce in intensity (*i.e.,* vertical thickness)).

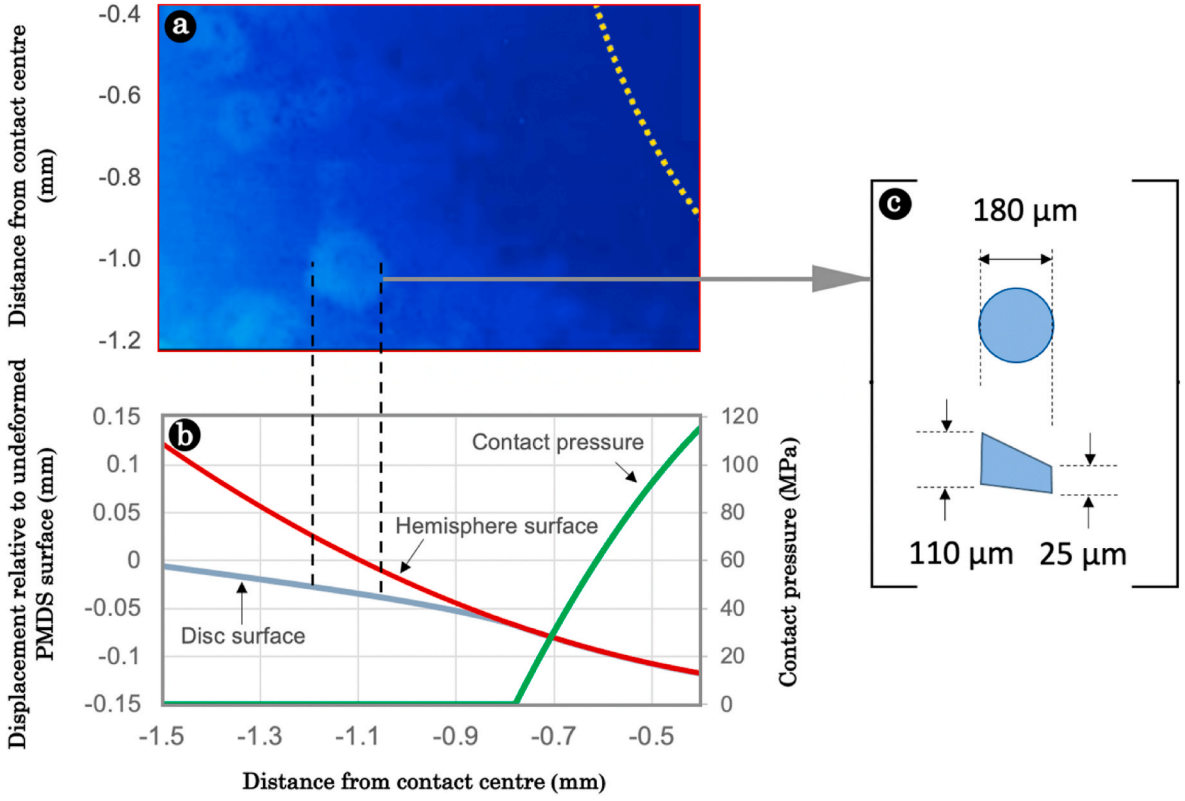

Fig. 10. a) Fluorescence image region of contact inlet for the dyed pea 1803 sample. Also see video in supplementary information. a) Particles located away from the contact are travelling with bulk fluid, b) calculated pin and disc surface geometry (red and blue respectively), Hertz contact pressure (green), c) detailed image of bubble geometry (note *x* and *y* axes scales are equal); c) dimensions of protein particle measured for (a) and (c). (For interpretation of the references to colour in this figure legend, the reader is referred to the Web version of this article.)

Agglomeration mechanism (Fan et al., 2011)). Then, following the addition of the astringent solution, these accumulated salivary particles are entrained through the contact, resulting in a rapid, short-lived decrease in friction.

The role of insoluble food protein particles entrainment in astringency is to cause abrasive wear that increases the average friction coefficient and contributes to significant frictional noise, which is likely to affect mouthfeel. A range of particle transport and deformation mechanisms occur as observed by in situ imaging.

These findings pave the way for the informed development of foods using plant-based and dairy proteins with increased popularity.

Statement of originality

1) The paper has not been published previously, that it is not under consideration for publication elsewhere, and that if accepted it will

not be published elsewhere in the same form, in English or in any other language, without the written consent of the publisher.
2) The paper does not contain material which has been published previously, by the current authors or by others, of which the source is not explicitly cited in the paper.

Declaration of competing interest

1) All authors have participated in (a) conception and design, or analysis and interpretation of the data; (b) drafting the article or revising it critically for important intellectual content; and (c) approval of the final version.
2) This manuscript has not been submitted to, nor is under review at, another journal or other publishing venue.
3) The authors have no affiliation with any organization with a direct or indirect financial interest in the subject matter discussed in the manuscript.

Data availability

Data will be made available on request.

Acknowledgments

This research was funded by Motif FoodWorks (Grant number P83696).

Appendix A. Supplementary data

Supplementary data to this article can be found online at https://doi.org/10.1016/j.foodhyd.2022.107975.

References

Adal, E., Sadeghpour, A., Connell, S., Rappolt, M., Ibanoglu, E., & Sarkar, A. (2017). Heteroprotein complex formation of bovine lactoferrin and pea protein isolate: A multiscale structural analysis. *Biomacromolecules, 18*(2), 625–635. https://doi.org/10.1021/acs.biomac.6b01857

Andoyo, R., Guyomarc'h, F., Cauty, C., & Famelart, M. H. (2014). Model mixtures evidence the respective roles of whey protein particles and casein micelles during acid gelation. *Food Hydrocolloids, 37*, 203–212. https://doi.org/10.1016/j.foodhyd.2013.10.019

Biegler, M., Delius, J., Käsdorf, B. T., Hofmann, T., & Lieleg, O. (2016). Cationic astringents alter the tribological and rheological properties of human saliva and salivary mucin solutions. *Biotribology, 6*, 12–20. https://doi.org/10.1016/j.biotri.2016.03.002

Bongaerts, J. H. H., Rossetti, D., & Stokes, J. R. (2007). The lubricating properties of human whole saliva. *Tribology Letters, 27*(3), 277–287. https://doi.org/10.1007/s11249-007-9232-y

Brossard, N., Cai, H., Osorio, F., Bordeu, E., & Chen, J. (2016). 'Oral' tribological study on the astringency sensation of red wines. *Journal of Texture Studies, 47*(5), 392–402. https://doi.org/10.1111/jtxs.12184

Carpenter, G., et al. (2019). A study of saliva lubrication using a compliant oral mimic. *Food Hydrocolloids, 92*. https://doi.org/10.1016/j.foodhyd.2019.01.049

Delwiche, J. (2004). The impact of perceptual interactions on perceived flavor. *Food Quality and Preference, 15*(2), 137–146. https://doi.org/10.1016/S0950-3293(03)00041-7

Drewnowski, A. (1997). Why do we like fat? *Journal of the American Dietetic Association, 97*, S58–S62.

Fan, J., Myant, C. W., Underwood, R., Cann, P. M., & Hart, A. (2011). Inlet protein aggregation: A new mechanism for lubricating film formation with model synovial fluids. *Proceedings - Institution of Mechanical Engineers Part H J. Eng. Med., 225*(7), 696–709. https://doi.org/10.1177/0954411911401306

Fan, N., Shewan, H. M., Smyth, H. E., Yakubov, G. E., & Stokes, J. R. (2021). Dynamic Tribology Protocol (DTP): Response of salivary pellicle to dairy protein interactions validated against sensory perception. *Food Hydrocolloids, 113*(July 2020), Article 106478. https://doi.org/10.1016/j.foodhyd.2020.106478

Fibrianto, K. (2013). *Contribution of anhydrous milk fat to oral processing and sensory perception of liquid milks*. The University of Queensland.

Gibbins, H. L., Proctor, G. B., Yakubov, G. E., Wilson, S., & Carpenter, G. H. (2014a). Concentration of salivary protective proteins within the bound oral mucosal pellicle. *Oral Diseases, 20*(7), 707–713. https://doi.org/10.1111/odi.12194

Gibbins, H. L., Yakubov, G. E., Proctor, G. B., Wilson, S., & Carpenter, G. H. (2014b). What interactions drive the salivary mucosal pellicle formation? *Colloids Surfaces B Biointerfaces, 120*, 184–192. https://doi.org/10.1016/j.colsurfb.2014.05.020

Hiiemae, K. M., & Palmer, J. B. (2003). Tongue movements in feeding and speech. *Critical Reviews in Oral Biology & Medicine, 14*(6), 413–429.

Humphrey, & Williamson, R. T. (2001). A review of saliva Normal composition, flow, and function. Humphrey, Williamson. 2001. Journal of Prosthetic Dentistry.pdf *The Journal of Prosthetic Dentistry, 85*(2), 162–169.

Jambrak, A. R., Mason, T. J., Lelas, V., Paniwnyk, L., & Herceg, Z. (2014). Effect of ultrasound treatment on particle size and molecular weight of whey proteins. *Journal of Food Engineering, 121*(1), 15–23. https://doi.org/10.1016/j.jfoodeng.2013.08.012

Janhoj, T., Frost, M. B., Prinz, J., & Ipsen, R. (2009). Sensory and instrumental characterization of low-fat and non-fat cream cheese. *International Journal of Food Properties, 12*(1), 211–227. https://doi.org/10.1080/10942910802252007

Kravchuk, O., Torley, P., & Stokes, J. R. (2012). No title. In B. Bhandari, & Y. H. Roos (Eds.), *Food materials science and engineering* (pp. 349–368). Wiley-Blackwell.

Labbe, D., Schlich, P., Pineau, N., Gilbert, F., & Martin, N. (2009). Temporal dominance of sensations and sensory profiling: A comparative study. *Food Quality and Preference, 20*(3), 216–221. https://doi.org/10.1016/j.foodqual.2008.10.001

Leksrisompong, P. P., Lopetcharat, K., Guthrie, B., & Drake, M. A. (2012). Descriptive analysis of carbonated regular and diet lemon-lime beverages. *Journal of Sensory Studies, 27*(4), 247–263. https://doi.org/10.1111/j.1745-459X.2012.00389.x

Malone, M. E., Appelqvist, I. A. M., & Norton, I. T. (2003). Oral behaviour of food hydrocolloids and emulsions. Part 1. Lubrication and deposition considerations. *Food Hydrocolloids, 17*(6), 763–773. https://doi.org/10.1016/S0268-005X(03)00097-3

McSweeney, P. L. H., & Fox, P. F. (2013). Advanced dairy chemistry, 4th ed.. In*Proteins: Basic aspects* (4th ed.„ *1A*. Boston, MA: Springer US

Meyer, D., Vermulst, J., Tromp, R. H., & De Hoog, E. H. A. (2011). The effect of inulin on tribology and sensory profiles of skimmed milk. *Journal of Texture Studies, 42*(5), 387–393. https://doi.org/10.1111/j.1745-4603.2011.00298.x

Myant, C., Reddyhoff, T., & Spikes, H.a. (2010). Laser-induced fluorescence for film thickness mapping in pure sliding lubricated, compliant, contacts. *Tribology International, 43*(11), 1960–1969. https://doi.org/10.1016/j.triboint.2010.03.013

Omrani Khiabanian, N., Motamedzadegan, A., Naghizadeh Raisi, S., & Alimi, M. (2020). Chemical, textural, rheological, and sensorial properties of wheyless feta cheese as influenced by replacement of milk protein concentrate with pea protein isolate. *Journal of Texture Studies, 51*(3), 488–500. https://doi.org/10.1111/jtxs.12508

Ortega-Requena, S., & Rebouillat, S. (2015). Bigger data open innovation: Potential applications of value-added products from milk and sustainable valorization of by-products from the dairy industry. *Green Chemistry, 17*(12), 5100–5113. https://doi.org/10.1039/c5gc01428j

Ployon, S., et al. (2018). Mechanisms of astringency: Structural alteration of the oral mucosal pellicle by dietary tannins and protective effect of bPRPs. *Food Chemistry, 253*(February), 79–87. https://doi.org/10.1016/j.foodchem.2018.01.141

Pons, M., & Fiszman, S. M. (1996). Instrumental texture profile analysis with particular reference to gelled systems. *Journal of Texture Studies, 27*(6), 597–624.

Prinz, J. F., de Wijk, R. A., & Huntjens, L. (2007). Load dependency of the coefficient of friction of oral mucosa. *Food Hydrocolloids, 21*(3), 402–408. https://doi.org/10.1016/j.foodhyd.2006.05.005

Reddyhoff, T., Underwood, R. J., Sayles, R. S., & Spikes, H. A. (2018). Temperature measurement of debris particles in EHL contacts. *Surface Topography: Metrology and Properties, 6*(3). https://doi.org/10.1088/2051-672X/aacf5a

Rossetti, D., Bongaerts, J. H. H., Wantling, E., Stokes, J. R., & Williamson, A. M. (2009). Astringency of tea catechins: More than an oral lubrication tactile percept. *Food Hydrocolloids, 23*(7), 1984–1992. https://doi.org/10.1016/j.foodhyd.2009.03.001

Rudge, R. E. D., Fuhrmann, P. L., Scheermeijer, R., van der Zanden, E. M., Dijksman, J. A., & Scholten, E. (2021). A tribological approach to astringency perception and astringency prevention. *Food Hydrocolloids, 121*, Article 106951. https://doi.org/10.1016/j.foodhyd.2021.106951

Sarkar, A., Ye, A., & Singh, H. (2016). On the role of bile salts in the digestion of emulsified lipids. *Food Hydrocolloids, 60*, 77–84. https://doi.org/10.1016/j.foodhyd.2016.03.018

Schiermeier, Q. (2019). Eat less meat: UN climate-change report calls for change to human diet. *Nature, 572*(291).

Selway, N., & Stokes, J. R. (2013). Insights into the dynamics of oral lubrication and mouthfeel using soft tribology: Differentiating semi-fluid foods with similar rheology. *Food Research International, 54*(1), 423–431. https://doi.org/10.1016/j.foodres.2013.07.044

Stokes, J. R. (2012). Food biopolymer gels, microgel and nanogel structures, formation and rheology. In B. Bhandari (Ed.), *Food materials science and engineering* (pp. 151–176). Wiley-Blackwell.

Stokes, J. R. (2012a). 'Oral' rheology. In J. Chen, & L. Engelen (Eds.), *Food oral processing: Fundamentals of eating and sensory perception* (pp. 227–263). Wiley Blackwell.

Stokes, J. R., Boehm, M. W., & Baier, S. K. (2013). Oral processing, texture and mouthfeel: From rheology to tribology and beyond. *Current Opinion in Colloid & Interface Science, 18*(4), 349–359. https://doi.org/10.1016/j.cocis.2013.04.010

Stokes, J. R., & Frith, W. J. (2008). Rheology of gelling and yielding soft matter systems. *Soft Matter, 4*(6), 1133–1140. https://doi.org/10.1039/b719677f

Troszyńska, A., Amarowicz, R., Lamparski, G., Wołejszo, A., & Baryłko-Pikielna, N. (2006). Investigation of astringency of extracts obtained from selected tannins-rich legume seeds. *Food Quality and Preference, 17*(1–2), 31–35. https://doi.org/10.1016/j.foodqual.2005.04.006

Vardhanabhuti, B., Cox, P. W., Norton, I. T., & Foegeding, E. A. (2011). Lubricating properties of human whole saliva as affected by β-lactoglobulin. *Food Hydrocolloids, 25*(6), 1499–1506. https://doi.org/10.1016/j.foodhyd.2011.02.021

de Vicente, J., Stokes, J. R., & Spikes, H. A. (2006). Rolling and sliding friction in compliant, lubricated contact. *Proceedings - Institution of Mechanical Engineers Part J J. Eng. Tribol., 220*(2), 55–63. https://doi.org/10.1243/13506501JET90

Vlădescu, S.-C. (2016). *The effects of surface texture in reciprocating bearings*. Imperial College London.

Vlădescu, S.-C., Ciniero, A., Tufail, K., Gangopadhyay, A., & Reddyhoff, T. (2017). Looking into a laser textured piston ring-liner contact. *Tribology International, 115*. https://doi.org/10.1016/j.triboint.2017.04.051

Vlădescu, S. C., et al. (2021). Effects of beverage carbonation on lubrication mechanisms and mouthfeel. *Journal of Colloid and Interface Science, 586*, 142–151. https://doi.org/10.1016/j.jcis.2020.10.079

Vladescu, S. C., Medina, S., Olver, A. V., Pegg, I. G., & Reddyhoff, T. (2016). Lubricant film thickness and friction force measurements in a laser surface textured reciprocating line contact simulating the piston ring-liner pairing. *Tribology International, 98*, 317–329. https://doi.org/10.1016/j.triboint.2016.02.026

Vladescu, S. C., Putignano, C., Marx, N., Keppens, T., Reddyhoff, T., & Dini, D. (2018). The percolation of liquid through a compliant seal-an experimental and theoretical study. *J. Fluids Eng. Trans. ASME, 141*(3), 1–12. https://doi.org/10.1115/1.4041120

de Wijk, R. A., Terpstra, M. E. J., Janssen, A. M., & Prinz, J. F. (2006). Perceived creaminess of semi-solid foods. *Trends in Food Science & Technology, 17*(8), 412–422. https://doi.org/10.1016/j.tifs.2006.02.005

Zeeb, B., et al. (2018). Modulation of the bitterness of pea and potato proteins by a complex coacervation method. *Food & Function, 9*(4), 2261–2269. https://doi.org/10.1039/c7fo01849e

Zembyla, M., et al. (2021). Surface adsorption and lubrication properties of plant and dairy proteins: A comparative study. *Food Hydrocolloids, 111*(July 2020), Article 106364. https://doi.org/10.1016/j.foodhyd.2020.106364